International Telecommunication Union

ITU-R

Radiocommunication Sector of ITU

Report ITU-R RS.2185
(10/2010)

Study on compatibility between "arrival time difference" (ATD) stations of the meteorological aids service and stations of the radionavigation service in the frequency band 9 to 14 kHz

RS Series

Remote sensing systems

International Telecommunication Union

Foreword

The role of the Radiocommunication Sector is to ensure the rational, equitable, efficient and economical use of the radio-frequency spectrum by all radiocommunication services, including satellite services, and carry out studies without limit of frequency range on the basis of which Recommendations are adopted.

The regulatory and policy functions of the Radiocommunication Sector are performed by World and Regional Radiocommunication Conferences and Radiocommunication Assemblies supported by Study Groups.

Policy on Intellectual Property Right (IPR)

ITU-R policy on IPR is described in the Common Patent Policy for ITU-T/ITU-R/ISO/IEC referenced in Annex 1 of Resolution ITU-R 1. Forms to be used for the submission of patent statements and licensing declarations by patent holders are available from http://www.itu.int/ITU-R/go/patents/en where the Guidelines for Implementation of the Common Patent Policy for ITU-T/ITU-R/ISO/IEC and the ITU-R patent information database can also be found.

Series of ITU-R Reports

(Also available online at http://www.itu.int/publ/R-REP/en)

Series	Title
BO	Satellite delivery
BR	Recording for production, archival and play-out; film for television
BS	Broadcasting service (sound)
BT	Broadcasting service (television)
F	Fixed service
M	Mobile, radiodetermination, amateur and related satellite services
P	Radiowave propagation
RA	Radio astronomy
RS	**Remote sensing systems**
S	Fixed-satellite service
SA	Space applications and meteorology
SF	Frequency sharing and coordination between fixed-satellite and fixed service systems
SM	Spectrum management

***Note**: This ITU-R Report was approved in English by the Study Group under the procedure detailed in Resolution ITU-R 1.*

Electronic Publication
Geneva, 2011

REPORT ITU-R RS.2185

Study on compatibility between "arrival time difference" (ATD) stations of the meteorological aids service and stations of the radionavigation service in the frequency band 9 to 14 kHz

(2010)

TABLE OF CONTENTS

1 Executive summary

This Report outlines the results of studies into the work seeking to define sharing criteria to manage compatibility between transmitting stations of the radionavigation services and passive arrival time difference (ATD) receivers operating in the meteorological service in the frequency band below 20 kHz.

It discusses various issues and aspects of VLF propagation and concludes on the sharing and regulatory management aspects of ATD sensors and radionavigation services within the frequency band under discussion.

The findings, reflecting the real life sharing environment for many years, are that sharing between both services is a high possibility and practicality. Notwithstanding the technical aspects discussed herein, this is partially due to the nature of deployment characteristics of both services, and interference mitigation implemented by the arrival time difference system of the meteorological aids service.

2 ATD and radionavigation station deployments at June 2010

Figure 1 shows the location of each of the existing ATD receiver locations (shown in green) and known RNAV transmitter locations (shown in red).

FIGURE 1

ATD receiver and RNAV transmitter locations

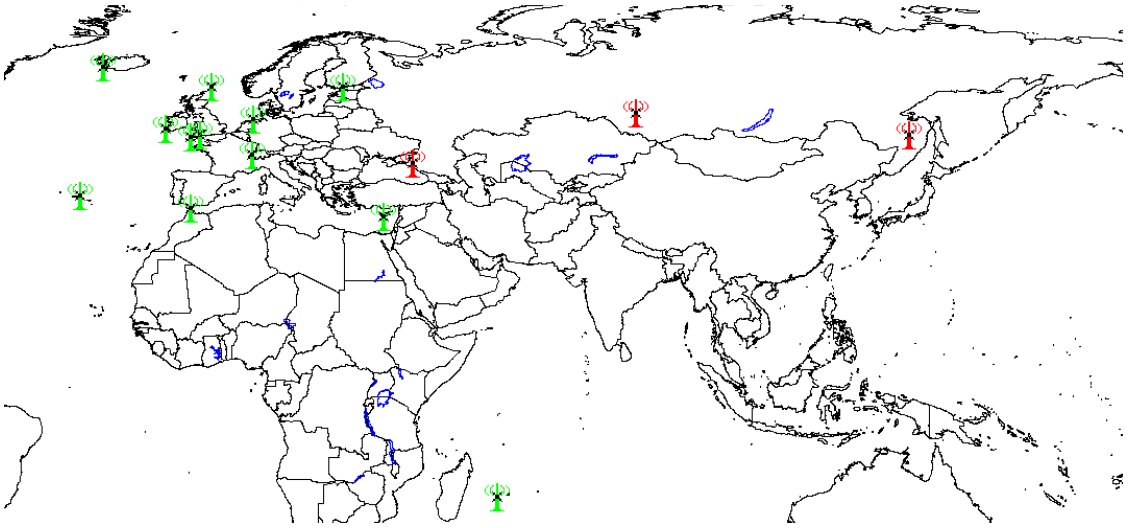

Report RS.2185-01

Actual ATD and RNAV site locations are shown in Tables 1 and 2.

TABLE 1

ATD receiver site locations

Site name	Latitude (decimal)	Longitude (decimal)
Valentia	51.939719N	10.244534W
Norderney	53.712421N	7.152314E
Exeter	50.728043N	3.475605W
Lerwick	60.139419N	1.185009W
Akrotiri	34.587151N	32.989052E
Gibraltar	36.152706N	5.348185W
Keflavik	63.968330N	22.614094W
Helsinki	60.203932N	24.961027E
La Reunion	20.896791S	55.485258E
Azores	38.658939N	27.223078W
Payerne	46.812123N	6.943854E
Camborne	50.218553N	5.327223W

TABLE 2

Radionavigation site locations

Site name	Latitude (decimal)	Longitude (decimal)
Komsomolsk Na Amure	50.5667N	136.96667E
Krasnodar	45.0333N	38.65E
Novosibirsk	55.0667N	82.9667E

3 Geographical separation between stations

The physical separation distance between each ATD receiver and each of the RNAV transmitters is also shown in Table 3.

TABLE 3

Separation distances between ATD and RNAV site locations

	Separation distance to RNAV site (km)		
ATD receiver site	**Komsomolsk Na Amure**	**Krasnodar**	**Novosibirsk**
Valentia	8 216	3 616	5 707
Norderney	7 520	2 453	4 668
Exeter	8 156	3 613	5 445
Lerwick	7 154	3 106	4 705
Akrotiri	7 994	1 259	4 428
Gibraltar	9 701	3 798	6 699
Keflavik	7 164	4 263	5 343
Helsinki	6 289	1 917	3 388
La Reunion	11 222	7 535	8 850
Azores	9 985	5 357	7 685
Payerne	8 185	2 446	5 141
Camborne	8 262	3 300	5 581

4 Typical radionavigation station parameters

The following section outlines various technical parameters of the radionavigation service.

4.1 RNAV transmitter characteristics

The parameters in Table 4 were used as being representative of a typical RNAV transmitter.

TABLE 4

Radionavigation stations parameters

Name of transmitting station	Occupied bandwidth (Hz)	Transmitting centre frequency (kHz)	Antenna input power (dBW)
Komsomolsk Na Amure	100, 200	11.905, 12.500, 12.649, 13.281, 14.881, 15.625	57
Krasnodar	100, 200	11.905, 12.500, 12.649, 13.281, 14.881, 15.625	57
Novosibirsk	100, 200	11.905, 12.500, 12.649, 13.281, 14.881, 15.625	57

4.2 RNAV antenna efficiency

The efficiency of a typical RNAV transmitting antenna at these frequencies is not known and is likely to be very small. Work by Raghuram *et al.* [1974], cites efficiencies of VLF transmitting antennas as low as 6 to 8% over a 3 000 m thick ice sheet, whereas over a conducting earth it is as low as 0.1% [1]. However references in declassified documents on the historical Omega system [2] provides efficiency values of the order of 10%. For these studies the radionavigation services have an assumed radiated power of 40 dBW. For radiated powers greater than 40 dBW, the required separation distances between stations shown in this study would be greater.

5 Typical ATD station parameters

Typical ATD station parameters are presented in Table 5.

TABLE 5

Typical ATD system parameters

Technical characteristics of the ATD system	
Receiver centre frequency	9.766 kHz
Receiver (sensor unit) amplifier gain	12 dB if switched on by control software (normally the case) otherwise zero [3]
Measurement bandwidth	3 kHz
Total “pass-band”	6.87 to 20.6 kHz
Antenna type and directivity	2 m vertical polarization, omnidirectional whip
Software filter	Broad-band high-pass filter (3 dB at 2.0 kHz), cascaded with low-pass filter (0.28 dB pass-band limit at 17.75 kHz)
Software narrow-band pass filter	3 dB bandwidth 2.5 kHz 10 dB bandwidth 4.3 kHz 20 dB bandwidth is 5.7 kHz
Typical receiver noise floor	–70.4 dBm in a 5 kHz reference bandwidth

6 Considerations of atmospheric noise

Recommendation ITU-R P.372-9 gives typical values for radio noise between 0.1 Hz and 100 GHz. Noting that in case of a ATD receiver the antenna is a 2 m monopole, used at frequencies where λ equates to between 25 to 38 km; equation (7) in this recommendation gives a suitable method to use to approximate levels of atmospheric noise at the input to this type of antenna.

Equation (7) provides the method, for a short (h << λ) vertical monopole, to calculate the r.m.s. vertical field-strength value of atmospheric noise above a perfect ground plane.

The equation is given by:

$$E_n = F_a + 20 \log f_{\mathrm{MHz}} + B - 95.5 \text{ dB}(\mu\text{V/m})$$

where:

E_n: field-strength in bandwidth b

f_{MHz}: centre frequency (MHz)

B: bandwidth of receiver

F_a: is the indicative value of atmospheric noise and is taken from Fig. 2.

FIGURE 2

F_a versus frequency (10^4 to 10^8 Hz)

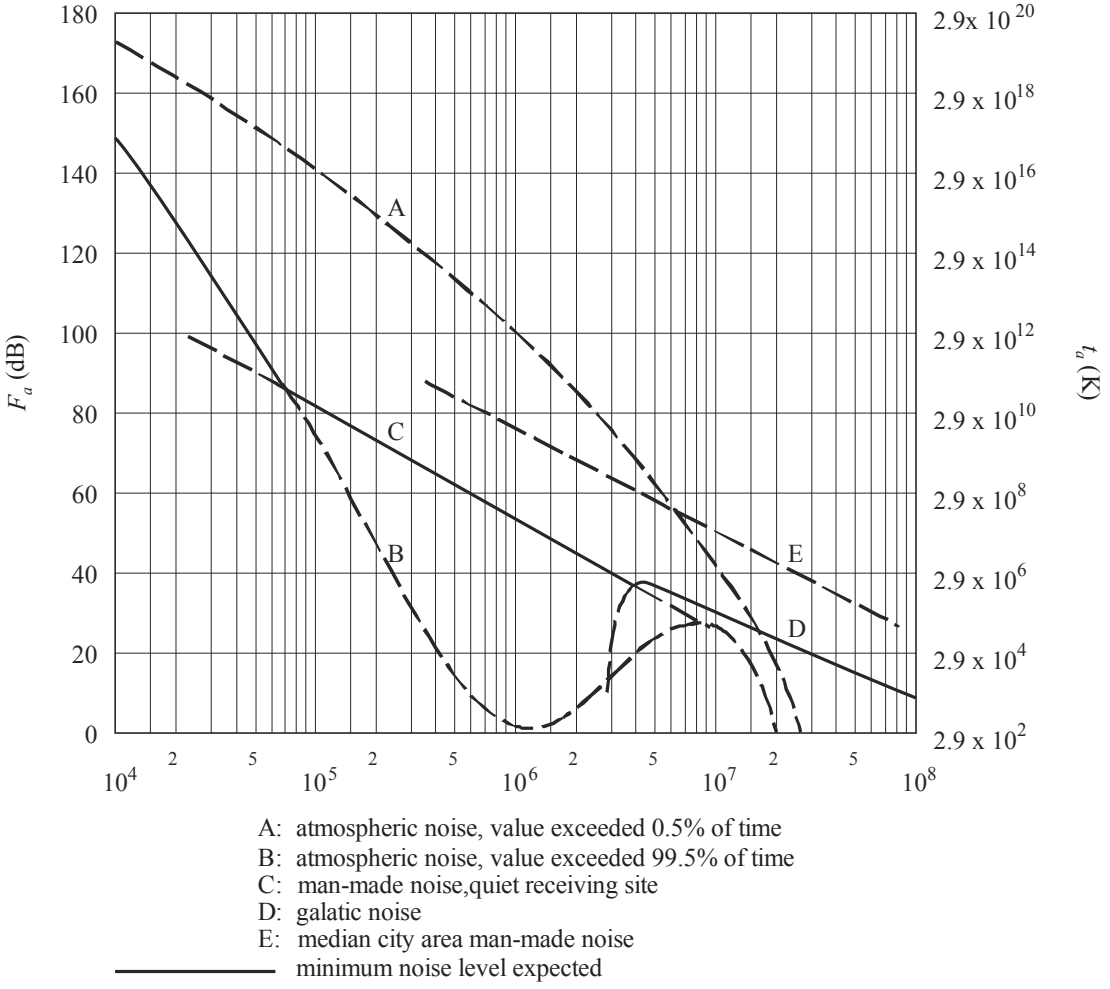

Report RS.2185-02

While Fig. 2 gives indicative values of atmospheric noise for 0.5% and 95% of the time, it is generalized and gives no information to their range of validity, especially regarding variances over geographical location, time and season. The same recommendation gives maps identifying expected values of F_{am} (median values of man-made noise power) (dB above KT_0b at 1 MHz, Figs 15a-38a) in different regions. In addition, it provides variation curves to assess the equivalent atmospheric noise values at other frequencies, in this case 10 kHz.

For example the values of F_{am} in wintertime over Europe range from 165 dB (04:00-08:00 h) to 151 dB (08:00-12:00 h). During spring time values of F_{am} are relatively constant until about 1 600 h where levels rise from about 155 dB to 162 dB.

The values of F_{am} for Hawaii correspond well with the values for Europe (within +/–5 dB).

In contrast, the values of F_{am} around Central Africa, Northern Australia and Malaysia show consistently higher values than those shown in Europe. During the period 16:00-20:00 h in the Summertime, F_{am} is as high as 172 dB, which is 10 dB higher than the highest values seen in Europe throughout the year.

Considering that the ATD sensor is limited by these variances in atmospheric noise, system performance is directly linked to the level of the atmospheric noise, therefore noise limited.

For example during times of high atmospheric noise levels the ATD system would not suffer performance limitations from interference from radionavigation service to the same degree as at those times or areas where atmospheric noise levels decreased by say 20 dB. This is point is especially important when the Earth-ionosphere wave guide effects on the interfering path do not vary to the same degree.

Considering that most ATD sensors are currently located in Europe and a high proportion of the origin of paths discussed in later sections within this paper are from Hawaii, the F_a value used in this study is 151 dB.

Using this assumption the atmospheric noise (E_n) at 9.766 kHz in a reference bandwidth of 3 kHz can be calculated as follows:

$$E_n = 151 + 20 \log (9\,766 \times 10^{-3}) + 10 \log (3\,000) - 95.5 \text{ dB}(\mu\text{V/m})$$

$$E_n = 50 \text{ dB}(\mu\text{V/m})$$

This value also corresponds to findings shown in ERC Report 069, which concludes that the levels of atmospheric noise field-strength levels at the 10 kHz range between 50-58 dB(μV/m) over a typical year within the European area.

Although 50 dB(μV/m) of atmospheric noise is the integrated effect of lightning strikes around the globe, and if localized lightning strikes were to occur the level would much higher; in this study 50 dB(μV/m) is taken to be the minimum wanted signal.

7 Interference mitigation

Notch filters are provided for removing the effects of interfering VLF radio transmissions primarily from sources other than the radionavigation services, which could in principle be highly coherent between outstations and could give rise to errors.

The software notch filter function has the form:

$$1\text{-}\exp(-(\Delta f/w)^2)$$

as indicated in Fig. 3 where:

f_0: the nominal frequency of the notch

Δf: the displacement of the frequency f from f_0

w: its width.

At the notch filter nominal frequency the signal is zeroed, but the reduction in signal becomes negligible at twice the notch width.

FIGURE 3

ATD sensor software filter function

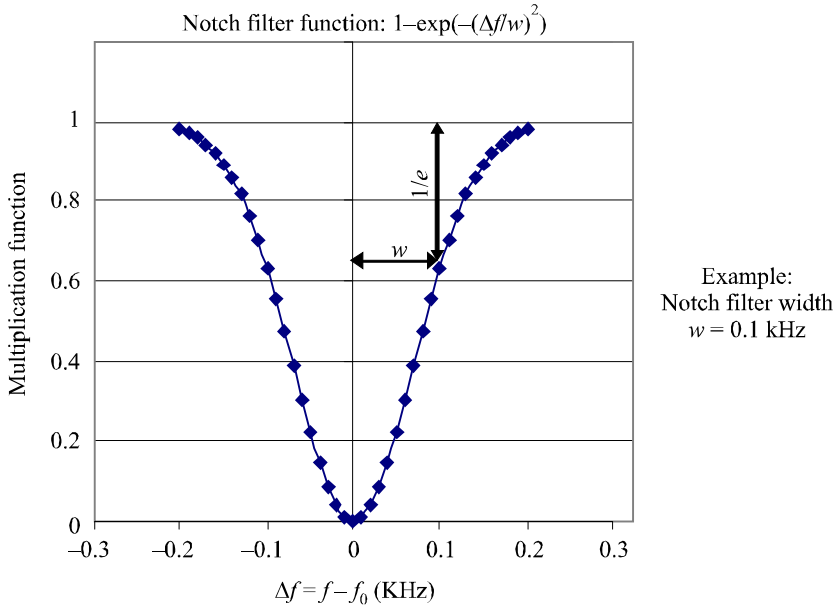

Report RS.2185-03

Considering the above notch filter function the typical attenuation that can be achieved for a 0.02 kHz and 0.2 kHz filter widths are 6 dB and 26 dB respectively.

The set up of notch filters of the same order can be seen in Fig. 4. In this example the measurement frequency is 13.766 kHz, with notch filters at 11.90 kHz (0.02 kHz), 12.65 kHz (0.02 kHz) and 16.4 kHz (0.2 kHz) (although these were not enabled when the screen shot was taken).

8 ATD receiver sensitivity and maximum permissible interference

Recommendation ITU-R RS.1881 specifies the minimum *C*/*I* values in respect to various frequency offsets from the ATD detection centre frequency. The following sharing study used the following assumptions:

– 50 dB(μV/m) as a minimum carrier level;

– Notch filtering implemented at 1, 2, 3, 4 and 5 kHz separation from measurement centre frequency, (notch filters of 0.02 kHz, 0.2 kHz, 0.2 kHz, 0.2 kHz and 0.2 kHz respectively).

From these assumptions the values for maximum field-strength of “I” can be derived for pulsed types of interferer. These are shown in Table 6.

FIGURE 4

Example of the an ATD sensor display

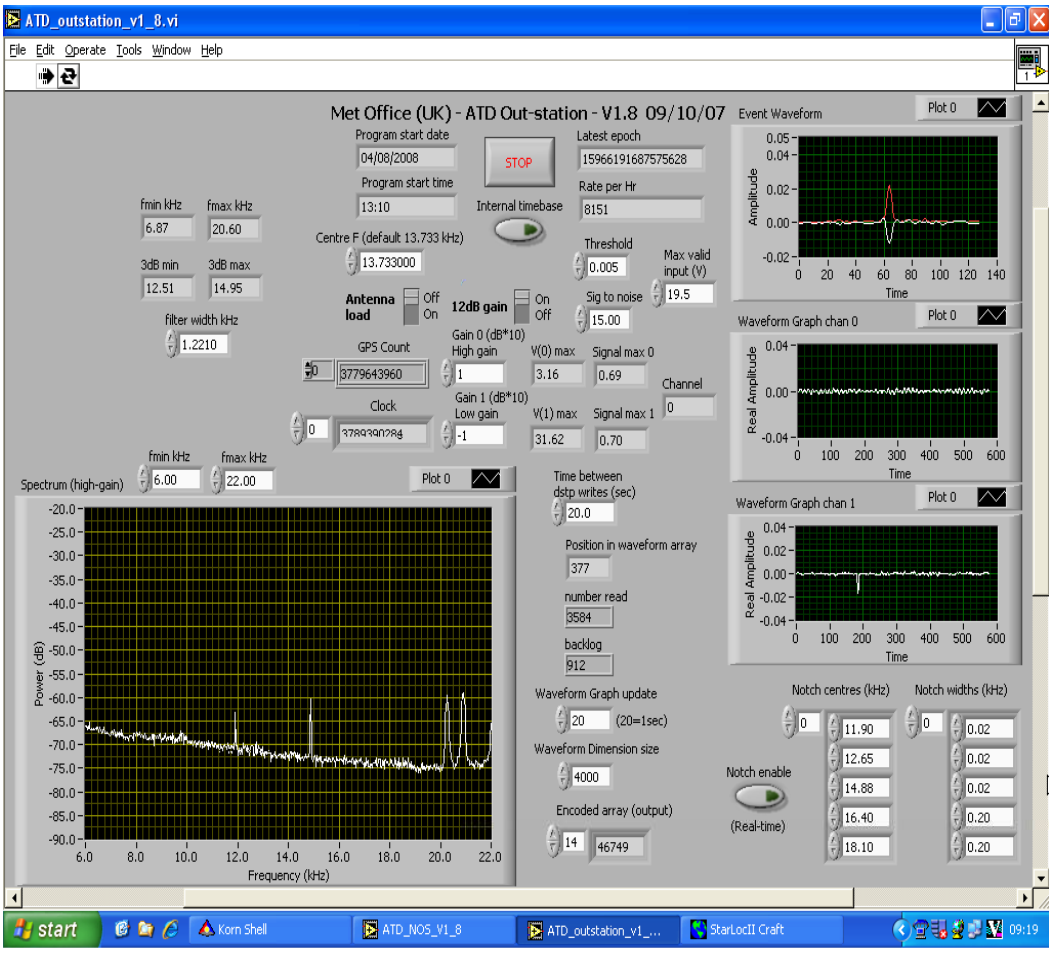

Report RS.2185-04

TABLE 6

Derived pulsed carrier wave (67% duty cycle) field-strength protection criteria at various frequency offsets from 9.766 kHz

Offset from 9.766 kHz (kHz)	Maximum permissible field-strength dB(μV/m)
–5	120
–4	107
–3	92
–2	59
–1	52
0	45
1	52
2	60
3	92
4	107
5	120

9 VLF propagation modelling

Propagation modelling at VLF frequencies is highly complex and dependent on various parameters such as characteristics of the ionosphere and density profile, geographical location, mode constants, propagation influences due to the geomagnetic dip and equator, day-night terminators, seasonal variations and sun spot activity.

Propagation at these frequencies can be represented in terms of waveguide theory, where the finitely conducting curved Earth and anisotropic, imperfectly conducting curved ionosphere with dipping magnetic fields form the boundaries of a wave guide within which signals at these frequencies can propagate to very great distances with minimal attenuation. This propagation phenomenon is characterized under the "*Earth-ionosphere wave guide*" theory. Although this complex theory is described in Recommendation ITU-R P.684, there is a clear absence of commercially available software tools that facilitate earth wave guide analysis.

Considering this sharing analysis is formed on the basis of two separate assessments:

– dominate mode earth wave guide theory;

– published historical VLF measurement and academic studies (including results from the historical FASTMC and LWPC computer programs).

9.1 VLF dominate mode theory

Although in Earth-ionosphere waveguide theory, the resultant field-strength will depend on the interaction of the various modes within the earth wave guide. On the basis of mode theory of VLF propagation as described by Wait [4], for distances greater than 2 000 km, the dominant mode can be considered to give a rough approximation of expected values of electric field-strength.

At distances $d > 2\,000$ km, the r.m.s. vertical electric field-strength field E at a great circle distance d from a transmitter, radiating power P(kW) is given by:

$$E \cong \frac{300}{h}\left[\frac{P\lambda}{\alpha \sin(d/a)}\right]^{1/2} \frac{e^{-ad_{mv}}}{m}$$

where:

a: the radius of the Earth

h: the height of the ionosphere reflecting layer (km)

λ: the wave length (km)

α: the attenuation factor (dB).

As the attenuation factor α is the only unknown factor for calculation of relative field-strength at Δd for a given transmitted power, by using data derived from real measurements, typical propagation attenuation factors for values $d > 2\,000$ km can be derived.

9.1.1 Historical VLF measurements deriving typical attenuation rates for various VLF path profiles

Using dominate mode theory and comparing empirical measurements work published by James R. Wait [5], A. P. Nickolaenko [6], Round, Eckersley, Tremellen & Lunnon [7] and C. J. Rodger *et al.,* [8] concluded the following night time attenuation factors shown in Table 7.

TABLE 7

Measured attenuation rates for various VLF transmission frequencies

Path geometry	Frequency of measurement (kHz)	Attenuation rate (dB) per 1 000 km at distances $d > 2\,000$ km	Tolerance (dB)
East-to-West (Atlantic)	Various (10 to 20)	2.6	Not stated
West-to-East (Atlantic)	Various (10 to 20)	2.1	0.3
North-to-South	Various (10 to 20)	2.5	0.2
Pacific Ocean (all sea path)	Various (10 to 20)	1.7	–0.7 / +1.3

It should be noted that daytime attenuation rates are generally far higher than those seen at night, in the order of increase of several dB's per 1 000 km. As this study looks at the worst case interference environment for interference received by radionavigation transmitters into ATD receivers, we need not consider or discuss daytime attenuation rates any further.

9.1.2 Generalizing attenuation as a factor of frequency and ground conductivity

Research by J. R. Wait [9] indicates the following theoretical results for dominant mode attenuation at distances greater than 2 000 km (see Fig. 5). The graphs indicate various attenuation rates as a factor of distance for paths of different ground conductivity values. It should be noted that these values generally agree with those shown in Table 7.

FIGURE 5

Typical attenuation rates verses frequency, ground conductivity and ionospheric parameters

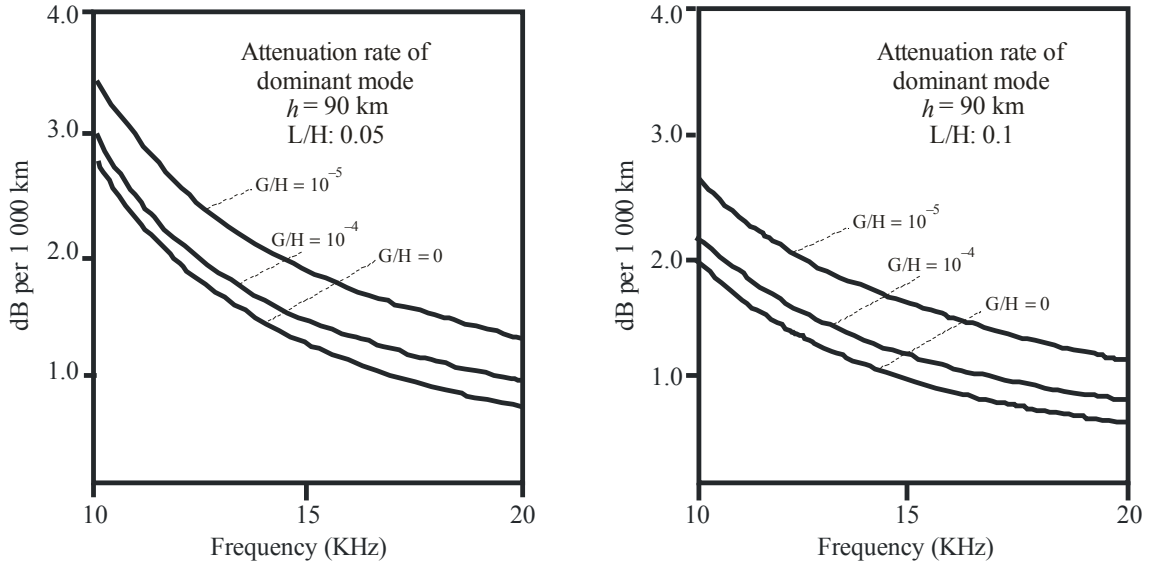

Report RS.2185-05

The two sets of curves shown represent attenuation for differing ionospheric conductivity values, where L/H is inversely proportional to the conductivity of the ionosphere. It has been suggested by Wait [10] that the best values of h and L/H for night time attenuation are 90 and 0.05 respectively. Values of ground conductivity values shown are of the following order: $G/H = 10^{-4}$ represents poor conducting land, $G/H = 10^{-5}$ represents well conducting land and G/H = 0 represents sea.

Although as stated by Wait [9] care is needed in assuming attenuation rates during transitions stages of a radio path between differing elements of ground conductivity (sudden changes to sea path from land paths can increase field-strength levels by up to 2 dB and are difficult to predict).

9.1.3 Sharing analysis using dominate mode theory by Wait [10]

As shown in § 9.1, on the basis of mode theory of VLF propagation as described by Wait [10], for distances greater than d >2 000 km, only the dominant mode need be considered in prediction of electric field-strength values.

At distances d >2 000 km, the r.m.s. vertical electric field-strength field E at a great circle distance d from a transmitter, radiating power P (kW) is given by:

$$E \cong \frac{300}{h}\left[\frac{P\lambda}{\alpha \sin(d/a)}\right]^{1/2} \frac{e^{-ad_{mv/m}}}{m}$$

where:

a: the radius of the Earth

h: the height of the ionosphere reflecting layer (km)

λ: the wave length (km)

α: the attenuation factor (dB).

Using the curves based on empirical measurements (shown in Fig. 5, § 9.1.3), the following attenuation rates shown in Table 8 can be derived.

TABLE 8

Typical attenuation rates for 11.905 and 12.5 kHz for various ground conductivity levels

	Attenuation rate (dB)	
Ground type	11.905 kHz	12.5 kHz
Poor conducting land	2.8	2.5
Good conducting land	2.3	2.0
Sea	2.0	1.8

Using the above theory predictive graphs can be derived illustrating typical field-strength levels at distances from 2 000 to 12 000 km from a hypothetical transmitter of 10 kW from 11.905 kHz and 12.5 kHz. These graphs are shown in the § 9.1.4.

9.1.4 Dominate mode graphs of predictive field-strength levels

Dominate mode graphs on predictive fields-strength levels for 10 kW transmitters are shown in Figs 6, 7, 8, 9, 10, 11.

FIGURE 6

Dominate mode 10 kW, 11.905 kHz. Path: land, G/H = 10^{-5} conductivity (good)

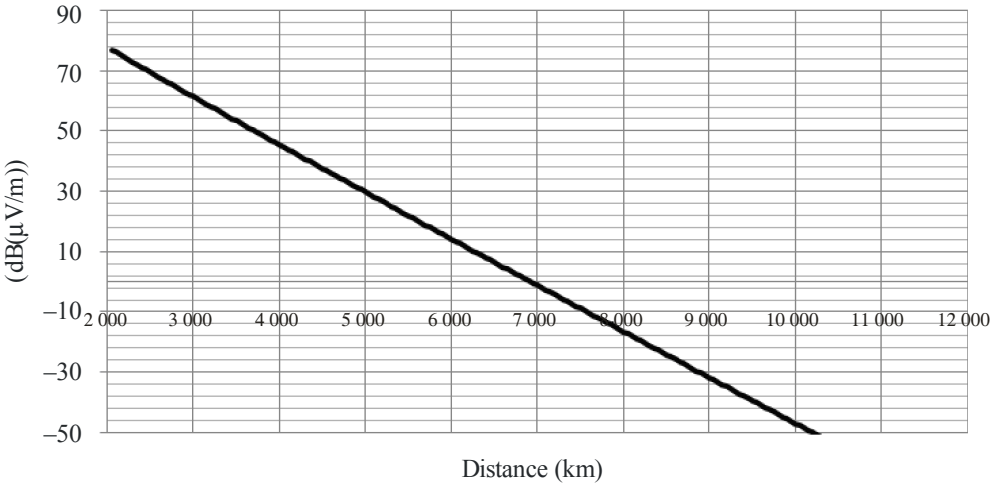

Report RS.2185-06

FIGURE 7

Dominate mode 10 kW, 11.905 kHz. Path: land, G/H = 10^{-4} conductivity (poor)

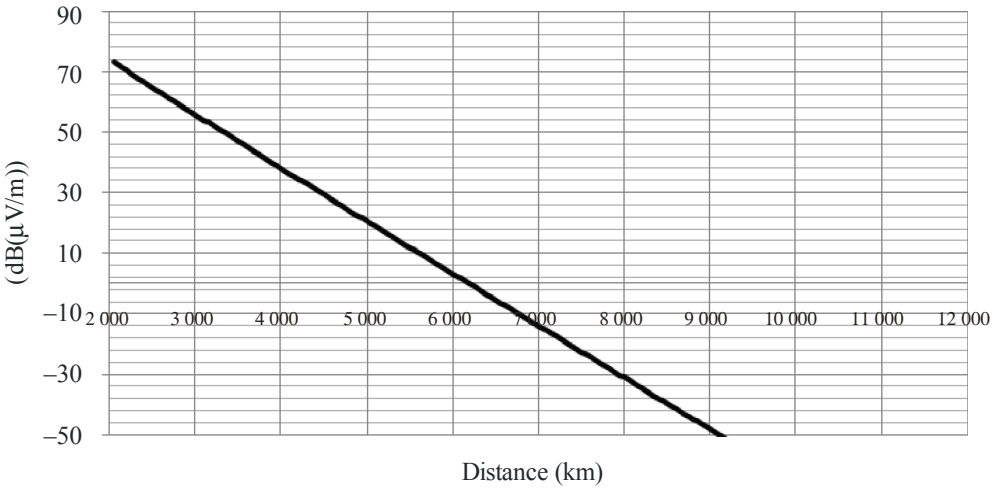

Report RS.2185-07

FIGURE 8

Dominate mode 10 kW, 11.905 kHz. Path: sea (G/H = 0 conductivity)

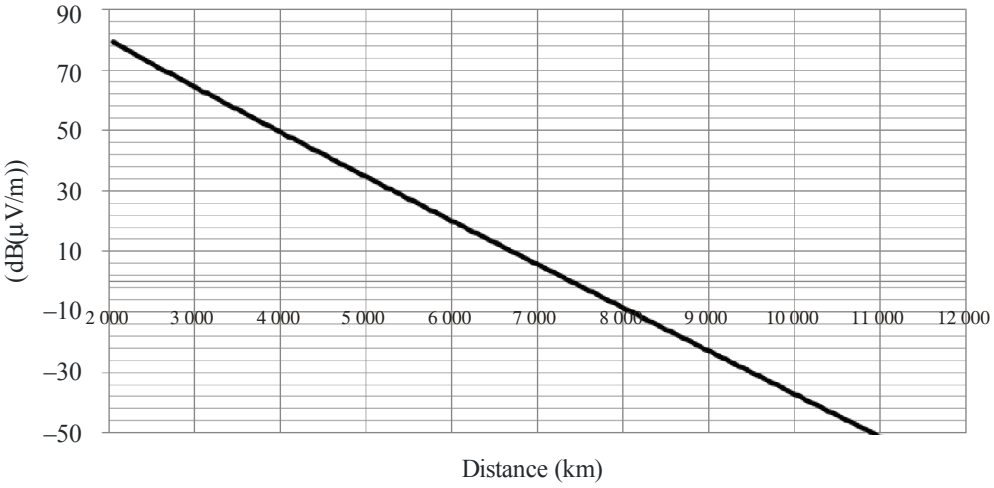

Report RS.2185-08

FIGURE 9

Dominate mode 10 kW, 12.5 kHz. Path: land, G/H = 10^{-5} conductivity (good)

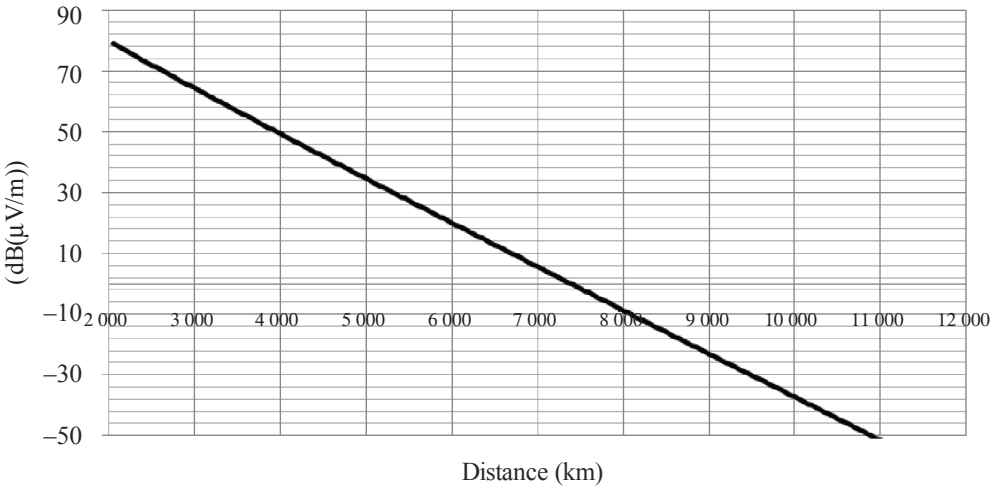

Report RS.2185-09

FIGURE 10

Dominate mode results 10 kW, 12.5 kHz. Path: land, G/H = 10^{-4} conductivity (poor)

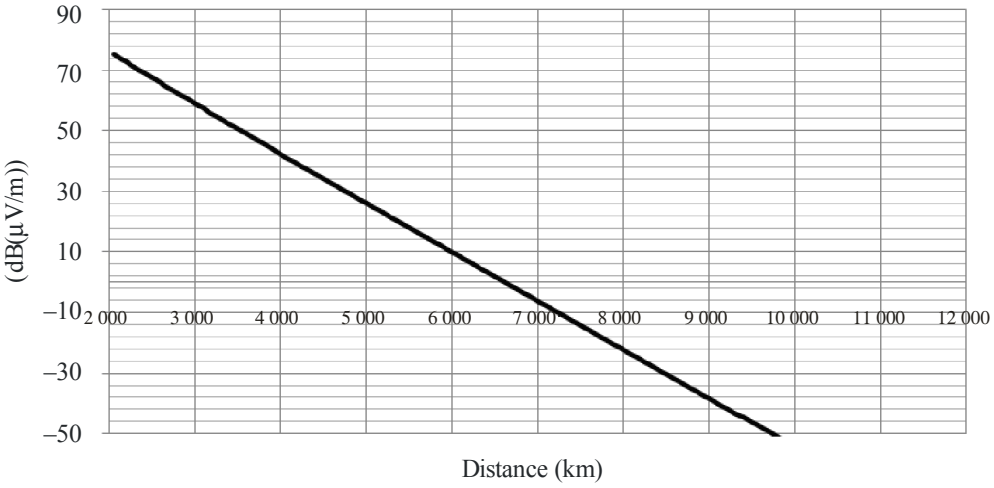

Report RS.2185-10

FIGURE 11

Dominate mode results 10 kW, 12.5 kHz, sea path (G/H = 0 conductivity)

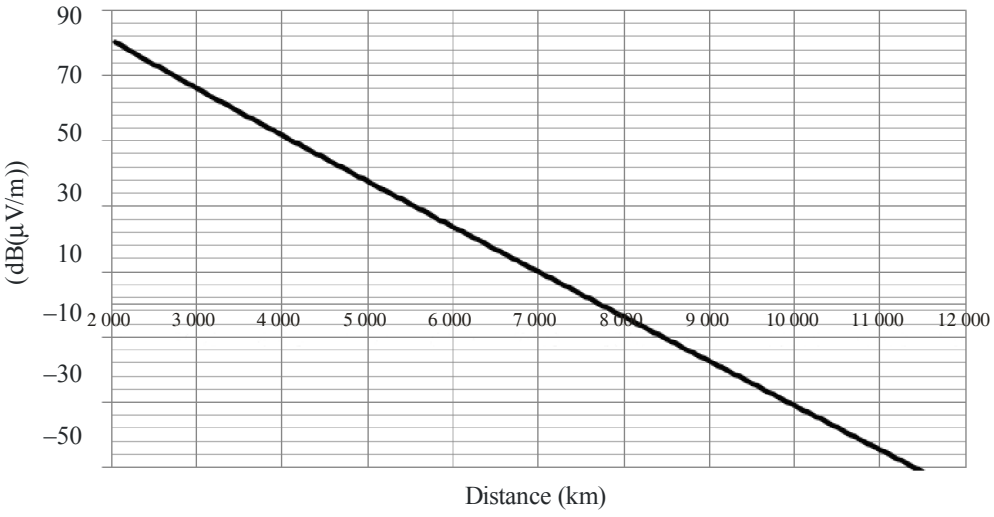

Report RS.2185-11

9.1.5 Dominate mode sharing analysis results

Using the graphs seen in § 10.2 and assuming the ATD sensor at 1 and 2 kHz frequency offset from the radionavigation centre frequency, the following necessary separation distances regarding compatibility between stations shown in Table 9 can be derived:

TABLE 9

Necessary separation distances between ATD sensors and radionavigation transmitters

Frequency (kHz)	Path type	Frequency offset (kHz)	Necessary separation distance (km)
11.905	Land (Poor, G/H =10^{-4})	1	3 300
11.905	Land (Good, G/H = 10^{-5})	1	3 600
11.905	Sea (G/H = 0)	1	3 900
11.905	Land (Poor, G/H = 10^{-4})	2	2 950
11.905	Land (Good, G/H = 10^{-5})	2	3 250
11.905	Sea (G/H = 0)	2	3 500
12.5	Land (Poor, G/H = 10^{-4})	1	3 500
12.5	Land (Good, G/H = 10^{-5})	1	3 850
12.5	Sea (G/H = 0)	1	4 050
12.5	Land (Poor, G/H = 10^{-4})	2	3 150
12.5	Land (good, G/H = 10^{-5})	2	3 450
12.5	Sea (G/H = 0)	2	3 600

For around 3 kHz separation between RNAV transmit and ATD measurement frequencies the necessary separation distance is less than 2 000 km. The exact distances are not possible to obtain by this method due to the limitations of dominate mode theory (dominate mode experiences greater interaction with other modes for distances less than 2 000 km from origin).

Additionally the use of notch filtering substantially improves the sharing possibilities between stations and dramatically reduces the distance between stations to co-exist. This reduction is of the order 12% for 1 kHz and > 50% for 2 kHz separation respectively.

9.2 Propagation of paths based on published research as a basis for compatibility between radionavigation services and ATD sensor stations

The following section illustrates and summarizes previously published research articles on VLF propagation in respect to radionavigation services. These articles cover both predicted and empirical measurements. Illustrations where available are provided with a brief description is given to any pertinent factors in relation to the plot under consideration. Finally these graphs/predictions are used

as a basis to inform findings on the necessary separation distances between radionavigation services and ATD stations of the meteorological aids service.

9.2.1 United States of America towards the Mediterranean

The following illustration is taken from previously published work by J.A. Ferguson [11] on predicted field-strength levels for a 10 kW transmitter located in the United States of America on a path towards the Mediterranean (see Figs 12, 13).

FIGURE 12

Propagation plots of an Omega transmission on 10.2 kHz, bearings 24° and 72°

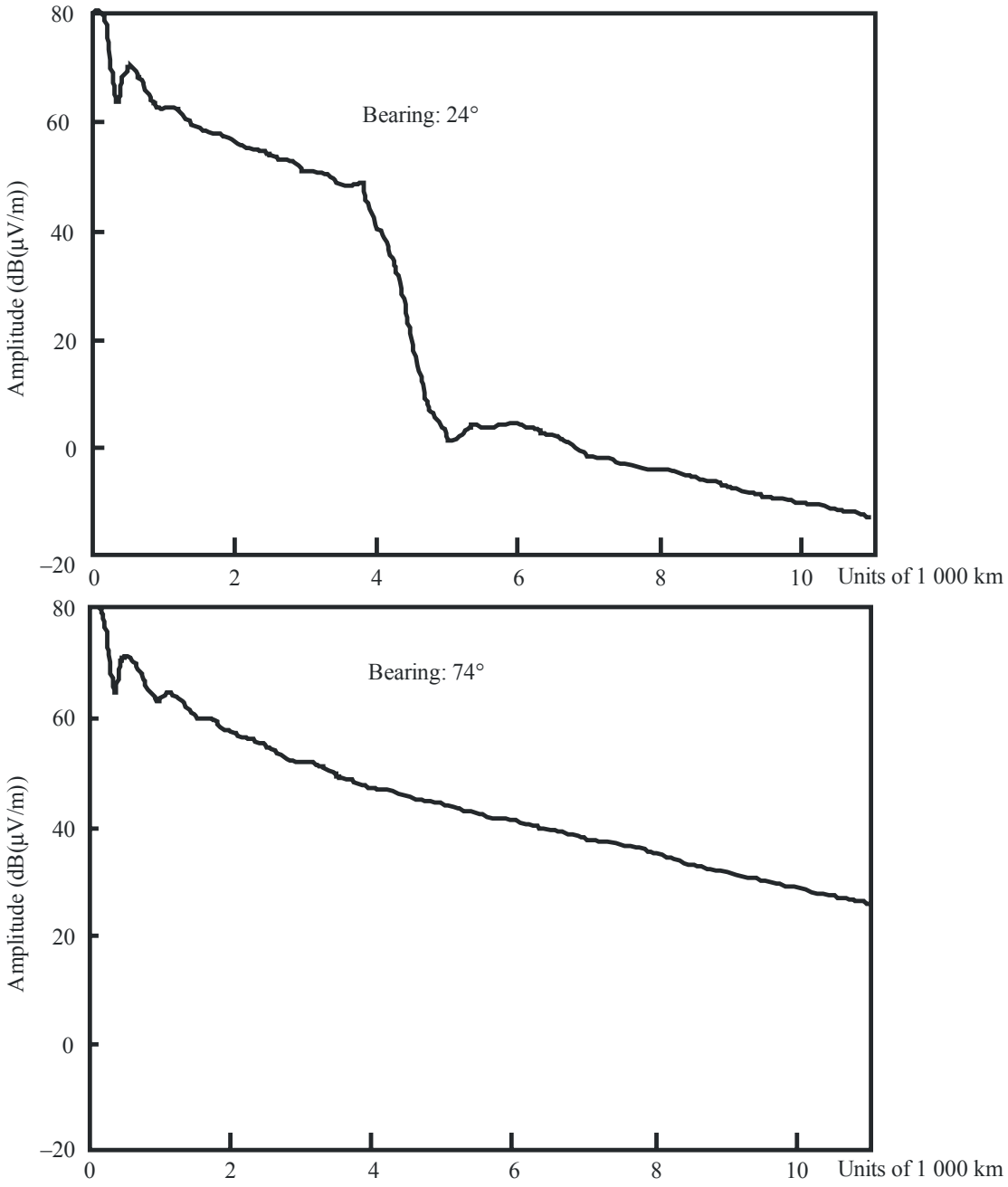

Report RS.2185-12

FIGURE 13

Propagation plots of an Omega transmission on 10.2 kHz, bearing 48°

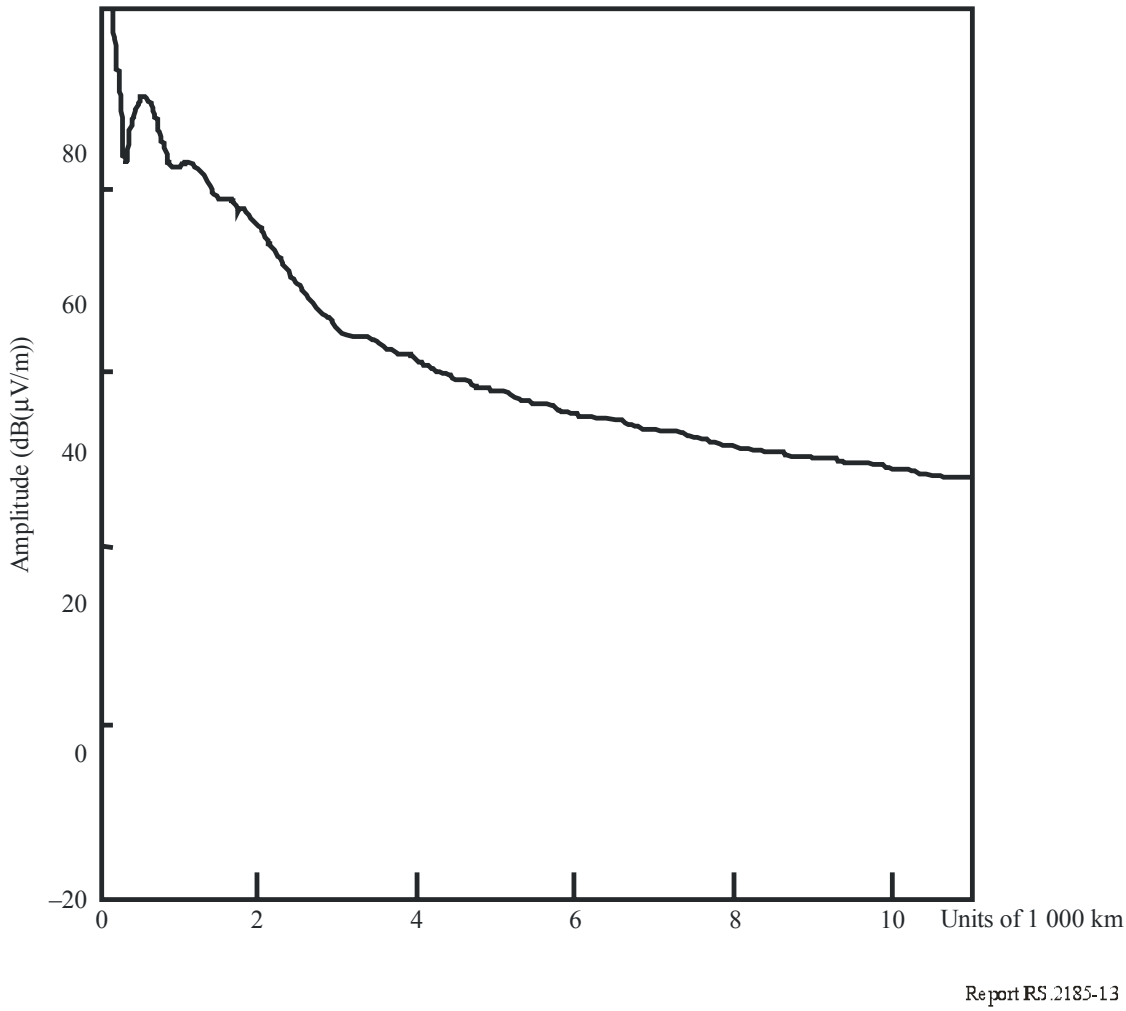

The above plots show a radio path based at 10.2 kHz for a transmit power of 10 KW from origin located at 46.4N, 98.3W (North Dakota). The first plot shows the path at a great circle bearing of 24° (North Easterly) over the Greenland ice cap. The second plot shows a path at great circle path of 72° (Easterly). The final plot shows a great circle path of 48°.

The first point of observation is that of the influence on the upper propagation path at around 4 000-4 500 km from origin this is due to the dielectric effects of the radio path over the Greenland icecap. The same situation is also evident in the second plot but to a lesser extent. Plots on 74° and 48° generally agree with the findings in Tables 7 and 8. Regarding the plot at 24°, the substantial reduction in field-strength shown at 4 000 km means this falls outside these generalizations of attenuation/1 000 km. It is also interesting to note that before the 4 000 km stage, the changes in angle of propagation path seem to have minimal effect on attenuation rate (±2B) (noting that all the plots have the same ground compositions up to this point).

9.2.2 CCIR measurements and empirical modelling

Figure 14 is taken from ITU CCIR Report 895-1 shows predicted and measured observations over the Pacific Ocean of a 1 kW transmission at night time from Hawaii to Southern California (East/West path) for various VLF frequencies. Each frequency plotted is plotted on the same graph, with 20 dB displacement between each of the frequencies.

FIGURE 14

Sea path attenuation various frequencies from Hawaii

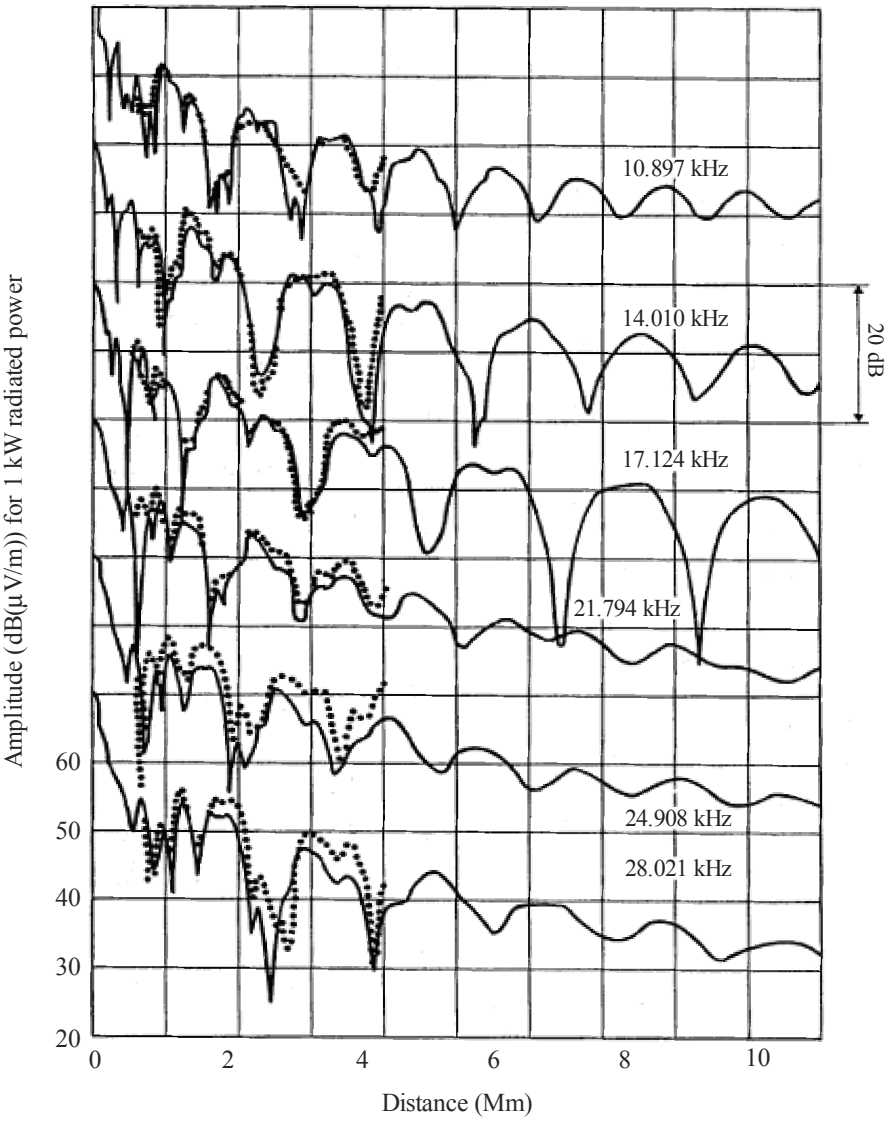

FIGURE 10 – *Propagation over the Pacific Ocean of signals transmitted from Hawaii to Southern California (night-time. winter)*

Predictions

Observations

Note – The amplitude scale applies to the lowest curve; the other curves are displaced 20 dB from each other.

Report RS.2185-14

It can be seen that for a pure sea path over the Pacific at night, for distances greater than 2 000 km the attenuation is approximately 10 dB over 8 000 km, equating to an average of 1.25 dB per 1 000 km. These figures agree with the values given in Tables 7 and 8.

9.2.3 Recommendation ITU-R P.684

This section outlines specific night time plots made from a transmitter based at Halifax in Canada on a bearing of 340° taken from Recommendation ITU-R P.684.

FIGURE 15

Field-strength verses distance taken from Recommendation ITU-R P.684

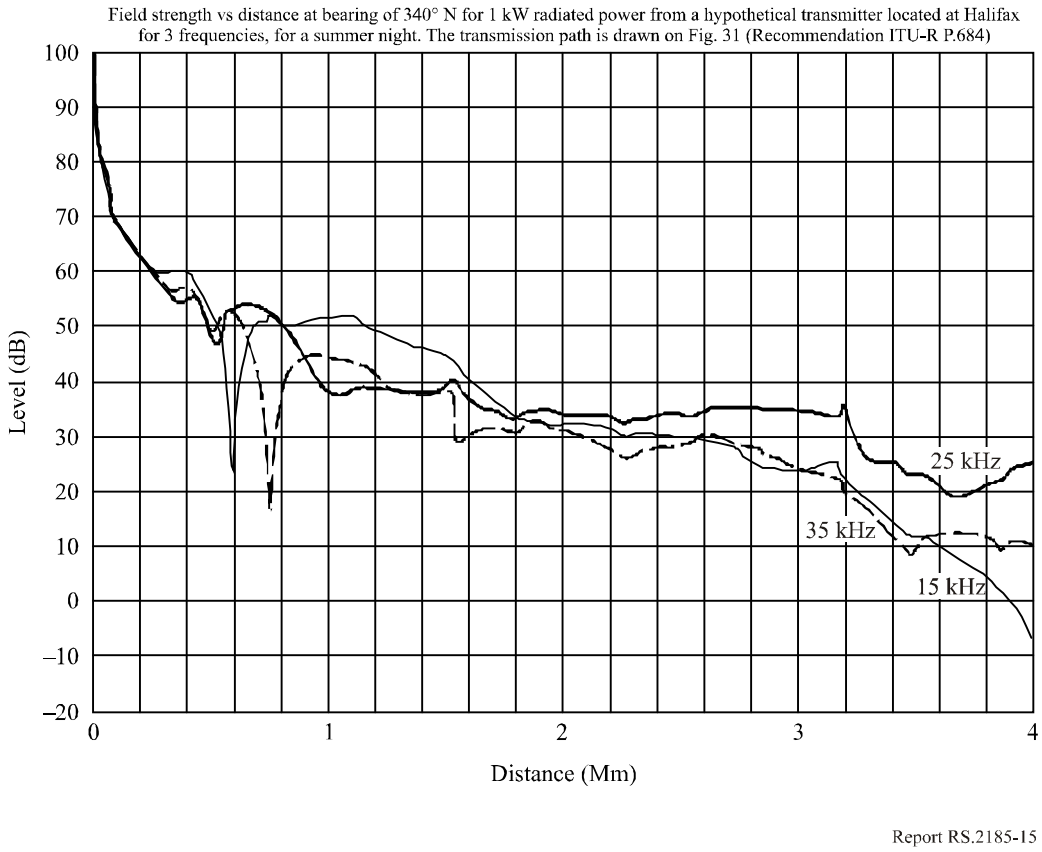

This north westerly path from Halifax at 340° is 1 000 km over a path with poor conductivity. The impact of the poor conducting land can be seen in the decrease of field-strength and high rate of attenuation.

9.2.4 Predictions using Recommendations ITU-R P.368 and ITU-R P.684 combined with results of historical measurements

An evaluation of the field-strength was performed on the basis of Recommendation ITU-R P.368 – Ground-wave propagation curves for frequencies between 10 kHz and 30 MHz. Figure 16 shows the calculation results of Alpha system signal field strength (E, dB(μV/m)) subject to distance (R) to receiving point.

The results shown above were obtained for ground wave propagation in accordance with Recommendation ITU-R P.368 for propagation over the land. These plots assume a transmitter e.r.p. of 57 dBW for frequencies of 10 kHz and 15 kHz.

Other calculation results were also assessed for propagation over sea and mixed paths, all of which were shown to be very similar for distances greater than 1 000 km. The differences between the obtained results were shown to be not greater than 3 dB.

FIGURE 16

Alpha system signal field-strength as a function of distance from transmitting antenna (R) for ground-wave propagation case

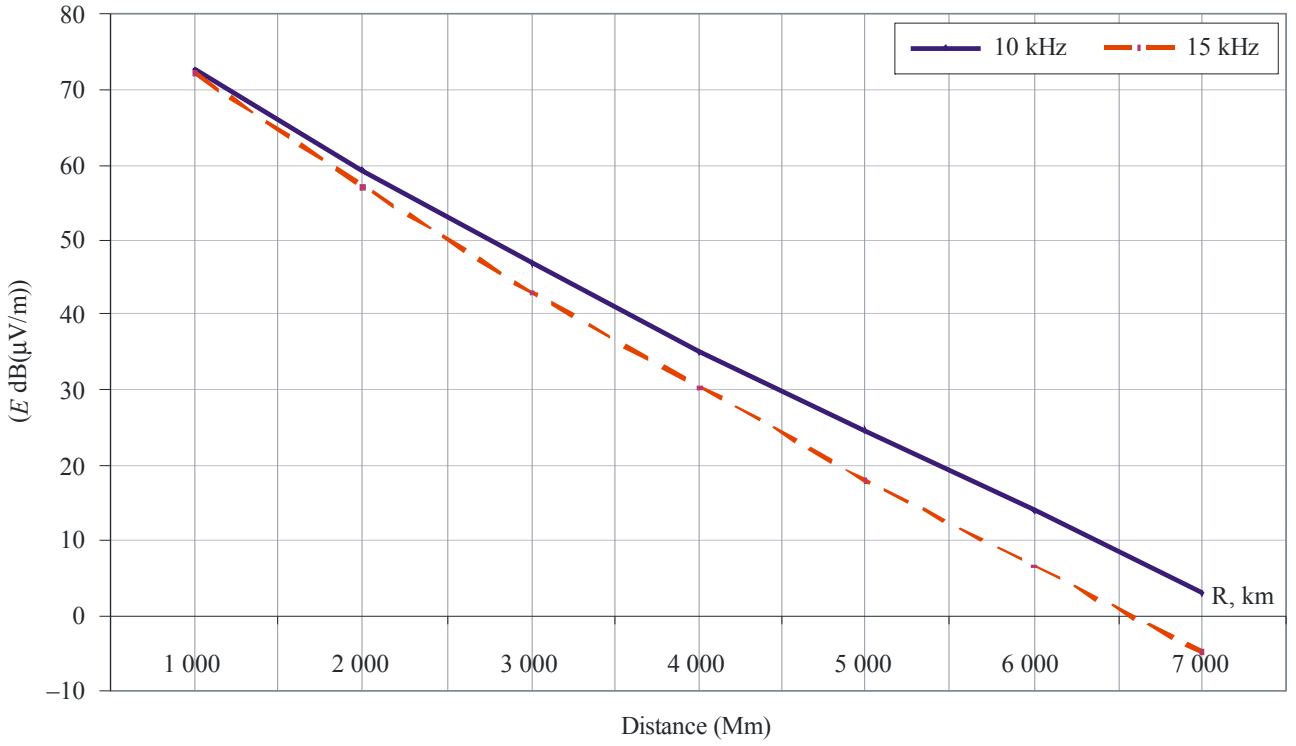

Figures 17 and 18 show the calculation results obtained for field-strength prediction using skywave propagation based on Recommendation ITU-R P.684 methodology combined with data from historical measurements. Assessment was made for frequencies of 10 kHz (see Fig. 17) and 15 kHz (see Fig. 18). Each frequency was assessed for day time and night time prediction shown in Figs (a) and (b) respectively.

In Figs 17 and 18, curve 1 represents the ground-wave component, curves 2, 3 and 4 represent skywave prediction, using assumptions of 4, 5 and 6 hops respectively.

FIGURE 17

Alpha system signal field-strength as a function of distance from transmitting antenna (R) for ground and ionosphere waves propagation case at 10 kHz

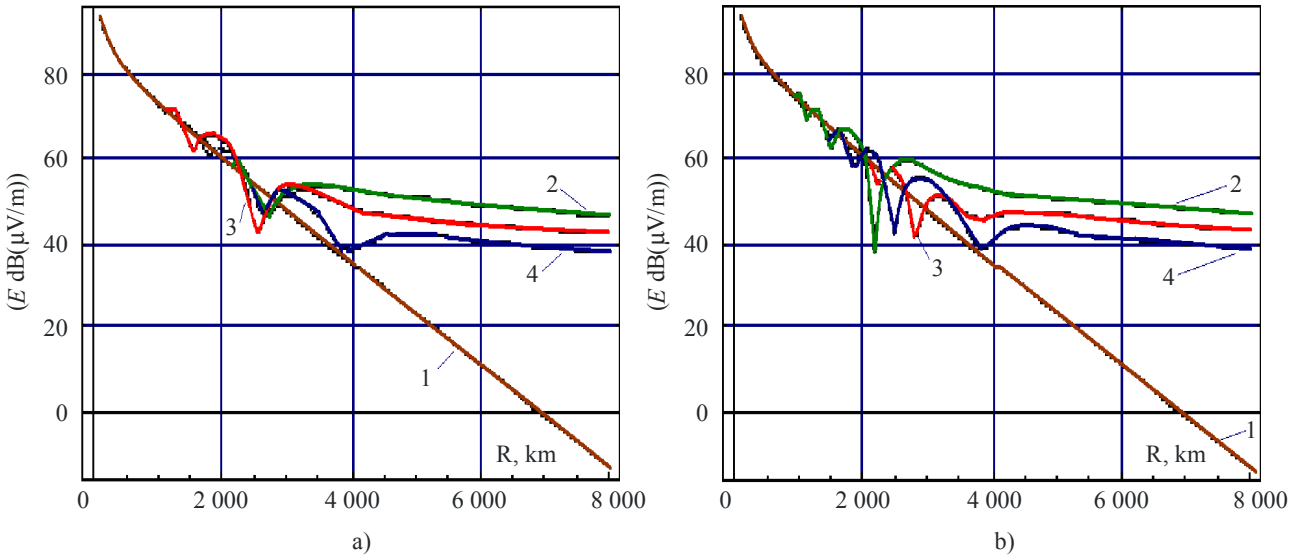

Report RS.2185-17

FIGURE 18

Alpha system signal field-strength as a function of distance from transmitting antenna (R) for ground and ionosphere waves propagation case at 15 kHz

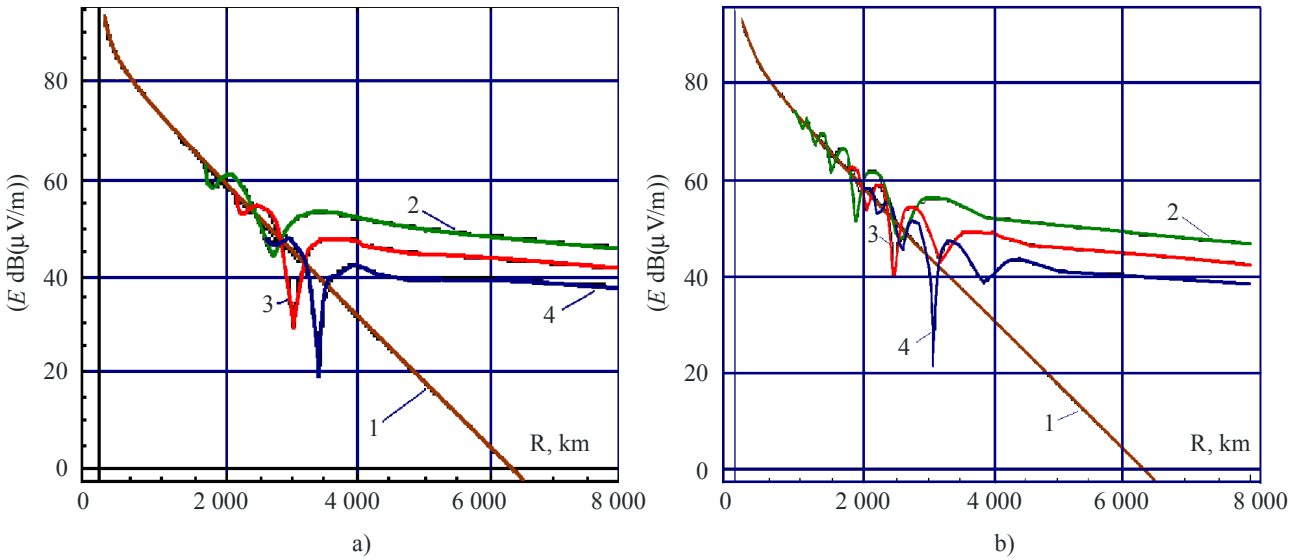

Report RS.2185-18

9.2.5 VLF measurements in the Pacific

The following plot outlines a path from a theoretical transmitter based at Hawaii on an east to west path to Tokyo [12] generated by Garner & Rhodes of NRL.

FIGURE 19

Propagation plot for 1 kW transmission from Hawaii towards Tokyo

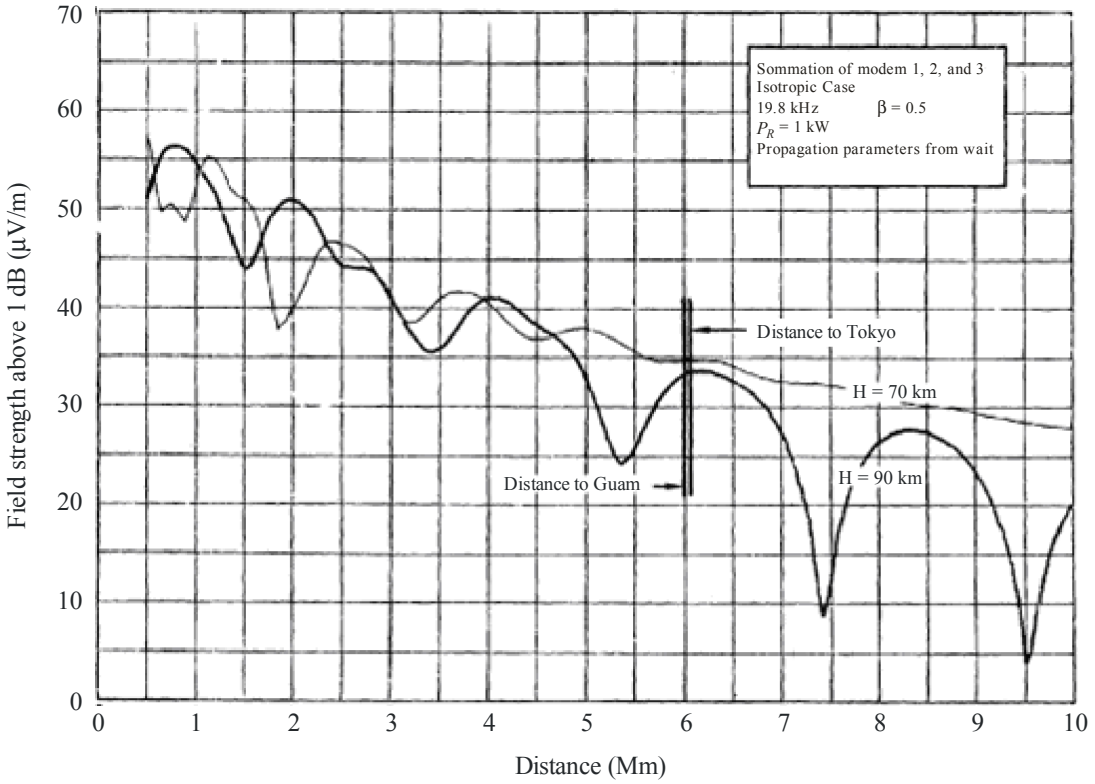

This diagram shows that for a 1 kW 19.8 kHz westerly path from Hawaii to Tokyo. Here it should be noted that between 7 000 and 9 000 km predicted field-strength level can vary in the order of 20 dB over 500 km.

9.2.6 Atlantic measurements by the Naval Ocean Systems Center

This section outlines articles published by various authors on measurements of the Omega radio navigation system.

Some of this work is based on actual measurements and some theoretical plots generated by the LWPC program.

Work executed by the Naval Ocean Systems Center [13] illustrated the measured and predicted attenuation loses for 16 kHz 65 kW VLF signals from the Rugby transmitter based in the UK. Measurements were on merchant ships during the period 1985 to 1986 on numerous sea paths to/from Europe and the United States of America (basic east-west paths). The some of the findings of work is shown in Table 10.

Work published by N.R. Thompson *et al.,* [14] on Omega VLF transmitters throughout the globe, focused on equatorial and non equatorial radio paths and their effects on propagation. The work cited averaged measurements made at night at various locations over the period May to June 1965. Some of their findings are shown in Table 11.

TABLE 10

Measured and predicted field-strength levels across the Atlantic for a 65 kW transmitter based at Rugby UK (16 kHz)

Measured/predicted	Season/time	Field-strength (dB(μV/m)) at 500 km	Field-strength (dB(μV/m)) at 1 000 km	Field-strength (dB(μV/m)) at 2 000 km
Measured	Autumn night	77	64	65
Measured	Winter night	78	65	65
Measured	Summer night	80	52	66
Measured	Spring night	79	67	66
Predicted (ionosphere height 87 km)	N/A	78	63	62
Predicted (ionosphere height 80 km)	N/A	75	67	66
Predicted (ionosphere height 84 km)	N/A	74	66	66

TABLE 11

Findings of equatorial and non equatorial Omega measurements

Transmitter Source and power	Transmitter power (kW)	Receiver location	Frequency (kHz)	Separation distance (km)	Average measured field-strength levels (dB(μV/m))
Omega Japan 34.6° N 129.5° E 28.0° N	10	Dunedin, NZ 45.9° S 170.5° E 53.1° S	13.6	9 800	43
Omega Japan 34.6° N 129.5° E 28.0° N	10	Dunedin, NZ 45.9° S 170.5° E 53.1° S	10.2	9 800	40
Omega Hawaii 21.5° N 157.8° W 21.5° N	10	Dunedin, NZ 45.9° S 170.5° E 53.1° S	11.8	8 100	30
Omega Hawaii 21.5° N 157.8° W 21.5° N	10	Dunedin, NZ 45.9° S 170.5° E 53.1° S	10.2	8 100	26

9.2.7 Results of sharing analysis using published VLF propagation data

Using the plots discussed in the previous section assessment was made on the necessary separation distance along the path illustrated, where the ATD Sensor could co-exist. All plots were normalized to assume radionavigation transmit powers of 10 kW. Additionally for each plot the ATD sensor was assumed to be at various frequency offsets to the radionavigation service centre frequency. These Offsets were of the order of 0 kHz, 1 kHz, 2 kHz and 3 kHz separation respectively. Comparison of predicted field-strength values from the graph were then made to the protection criteria shown in § 8, Table 6.

The findings of this initial analysis are shown in Table 12.

TABLE 12

Analysis of necessary separation distance between radionavigation transmitters based on published VLF propagation data

Plot name	Frequency	Transmit power (kW)	Direction of path	Path type	ATD frequency offset to plot frequency (kHz)	General Coexistence separation distance (km)
Hawaii to Southern California	10.897	10	East	Sea	0	Not compatible
Hawaii to Southern California	10.897	10	East	Sea	1	> 6 800
Hawaii to Southern California	10.897	10	East	Sea	2	> 4 700
Hawaii to Southern California	10.897	10	East	Sea	3	No data available
Hawaii to Southern California	14.010	10	East	Sea	0	Not compatible (excluding nulls)
Hawaii to Southern California	14.010	10	East	Sea	1	> 6 250
Hawaii to Southern California	14.010	10	East	Sea	2	> 4 600
Hawaii to Southern California	14.010	10	East	Sea	3	No data available
N Dakota to Med	10.2	10	East (24°)	Land. Sea, land	0	> 4 000
N Dakota to Med	10.2	10	East (24°)	Land. Sea, land	1	> 3 000
N Dakota to Med	10.2	10	East (24°)	Land. Sea, land	2	> 1 800
N Dakota to Med	10.2	10	East (24°)	Land. Sea, land	3	> 100
N Dakota to Med	10.2	10	East (72°)	Land. Sea, land	0	> 4 700
N Dakota to Med	10.2	10	East (72°)	Land. Sea, land	1	> 2 900

TABLE 12 (*end*)

Plot name	Frequency	Transmit power (kW)	Direction of path	Path type	ATD frequency offset to plot frequency (kHz)	General Coexistence separation distance (km)
N Dakota to Med	10.2	10	East (72°)	Land. Sea, land	2	> 2 100
N Dakota to Med	10.2	10	East (72°)	Land. Sea, land	3	> 100
N Dakota to Med	10.2	10	East (48°)	Land. Sea, land	0	> 3 000
N Dakota to Med	10.2	10	East (48°)	Land. Sea, land	1	> 2 500
N Dakota to Med	10.2	10	East (48°)	Land. Sea, land	2	> 1 800
N Dakota to Med	10.2	10	East (48°)	Land. Sea, land	3	> 100
Halifax 340°	15.0	10	NW	Land	0	> 1 800
Halifax 340°	15.0	10	NW	Land	1	> 1 600
Halifax 340°	15.0	10	NW	Land	2	> 1 250
Halifax 340°	15.0	10	NW	Land	3	> 100
Hawaii – Tokyo	19.8	10	Westerly	Sea	0	> 4 800
Hawaii – Tokyo	19.8	10	Westerly	Sea	1	> 2 900
Hawaii – Tokyo	19.8	10	Westerly	Sea	2	> 2 250
Hawaii – Tokyo	19.8	10	Westerly	Sea	3	No data available
Rugby to USA	16.0	10	Westerly	Sea	0	> 6 500
Rugby to USA	16.0	10	Westerly	Sea	1	> 3 600
Rugby to USA	16.0	10	Westerly	Sea	2	> 2 250
Rugby to USA	16.0	10	Westerly	Sea	3	> 100

9.2.8 Published VLF propagation data sharing analysis results

For the radio paths discussed in § 11. Assuming a radionavigation service transmitter operating on a 10 kW (transmit power) and an atmospheric noise level of 50 dB(μV/m) the following conclusions can be made.

The use of notch filtering substantially mitigates the impact of unwanted radionavigation emissions to ATD sensor detection and reduces necessary separation distances between stations by as much as > 30% at 2 kHz and 75% at 3 kHz separation from ATD measurement frequency.

Assuming implementation of notch filters based at 2 kHz and 3 kHz from ATD measurement frequency the following can be seen regarding necessary separation distances between stations:

– for north westerly paths over poor conducting land, the separation distances are of the order of 1 600 km at 1 kHz frequency offset, 1 250 km at 2 kHz and 100 km at 3 kHz respectively;

– for northerly mixed paths (land sea land), the separation distances are of the order of 2 500-3 000 km at 1 kHz frequency offset, 1 800-2 100 km at 2 kHz and 100 km at 3 kHz respectively;

– for easterly sea paths the separation distances are of the order of 6 250-6 800 km at 1 kHz frequency offset, 4 600-4 700 km at 2 kHz respectively;

– for westerly sea paths the separation distance are of the order of 2 900-3 600 km at 1 kHz frequency offset, 2 500 km at 2 kHz and 100 km at 3 kHz respectively.

Additionally, through the selective selection of ATD sensor sites, this could reduce the necessary separation distances between stations further. Even in cases where 90% of a path exceeds the ATD sensor threshold selective selection of a sensor location would make compatibility a possibility (locating of sensors at nulls formed due to modal interaction within the Earth-ionosphere waveguide).

10 Conclusions on sharing between the radionavigation services and ATD sensors of the meteorological aids service

Co-existence and sharing between the radionavigation service and ATD sensors has been shown to be possible, not only from a theoretical basis as seen in this document but in practice also.

From a technical perspective the necessary separation distances are found to be of the following order:

TABLE 13

Necessary separation distances based on 10 kW radionavigation e.i.r.p.

Path dielectric	Frequency offset from ATD measurement frequency (kHz)	Separation distance (km)
Land Good (Good, G/H = 10^{-5})	1	2 500-3 850*
Land Poor (G/H = 10^{-4})	1	1 600-3 500*
Sea (westerly) Sea (G/H = 0)	1	2 900-3 900*
Sea (Easterly Sea (G/H = 0)	1	3 900-6 800*
Land Good (Good, G/H = 10^{-5})	2	1 800-3 450*
Land Poor (G/H = 10^{-4})	2	1 250-3 150*
Sea (westerly) Sea (G/H = 0)	2	2 250-3 600*

TABLE 13 (*end*)

Path dielectric	Frequency offset from ATD measurement frequency (kHz)	Separation distance (km)
Sea (Easterly Sea (G/H = 0)	2	3 500-4 700
Land Good (Good, G/H = 10^{-5})	3	100
Land Poor (G/H = 10^{-4})	3	100
Sea (westerly) Sea (G/H = 0)	3	No information available
Sea (Easterly) Sea (G/H = 0)	3	No information available

* Those upper distances marked "*" are worst case derived from dominate mode propagation theory and are unlikely to be fully representative of real life sharing scenarios, which are likely to be lower.

From practical experience the two services have co-existed since 1989 with no impact to either service, even with a geographically dispersed ATD sensor network throughout the globe. In cases whereby close proximity between stations occurs (minimum distance between services today is 1 048 km), the effective implementation of notch filtering is sufficient to allow the two services to co-exist at 1 kHz frequency offset. Noting that historically with the Omega system, effective ATD sensor operations were possible on 9.766 kHz with transmissions on 10.2 kHz, at a separation distance of only 973 km over a sea path. This in part was possible due to short pulse widths of radionavigation transmissions (0.2 s) and separation between pulses of 9 s intervals.

It can be concluded, given the nature of radionavigation services and ATD sensors operating in this frequency band, the low density levels and static nature of station deployments, and this environment was to continue, that effective sharing between these services is a high possibility and practicality with little constraints placed on either service.

References

[1] WATT, A. D. VLF Engineering.

[2] VALLESE, L. M., PASSALAQUA, A. M., RAKOWSKY, G, Solid State Devices Applications for ASW. VLF Ferrite Antennas, ITT Federal Labs Nutley NJ ITT.

[3] The 12 dB amplifier gain is used for long range detection, in the event of lightning strikes being in close proximity to the receiver, input gain is reduced to zero.

[4] WAIT, J. R. [1957] The mode theory of VLF propagation. Geofisica pura e applicata, Milano, Vol. 37, p. 103-115.

[5] WAIT, J. R. [1958] National Bureau of standards, Boulder, Colorado USA and NICKOLAENKO, A. P. [1989].

[6] NICKOLAENKO, A. P. [1989] ELF/VLF propagation measurements in the Atlantic during 1989.

[7] Round, Eckersley, Tremellen & Lunnon [1925] Report on measurements made on signal strength at great distances during 1922 and 1923 by expedition sent to Australia. Journal of Electrical Engineers, Vol. 63, p. 933, 1011.

[8] ROGER, C. J., BRUNDELL, J. B., DOWDEN, R. L. and THOMSON, N. R [2004] Location accuracy of long distance VLF lightning location network. Department of Physics University of Otago, New Zealand, European Geosciences Union.

[9] WAIT, J. R. [1958] A study of VLF field-strength data: Both old and new, Istituto Geofisico Italiano, Milano.

[10] WAIT, J. R. [1957] The mode theory of VLF propagation. Geofisica pura e applicata, Milano, Vol. 37, p. 103-115.

[11] FERGUSON, J. A. [1998] Computer Programs for assessment of long wavelength radio communications version 2.0, SPAWAR Center San Diego CA 92152-5001 p. 41.

[12] MAXWELL, E. L. [1966] VLF measurements in the Pacific, p. D-2.

[13] FERGUSON, J. A. [1992] A review of the ionospheric model for the long wave prediction capability.

[14] THOMSON, Neil R. and WAYNE, M. McRae [1965] Night time Ionospheric D-region: Equatorial and non-equatorial.